A comparison of methods for melting point calculation using molecular dynamics simulations

Yong Zhang, and Edward J. Maginn

Citation: The Journal of Chemical Physics **136**, 144116 (2012);
View online: https://doi.org/10.1063/1.3702587
View Table of Contents: http://aip.scitation.org/toc/jcp/136/14
Published by the American Institute of Physics

A comparison of methods for melting point calculation using molecular dynamics simulations

Yong Zhang and Edward J. Maginn[a)]
Department of Chemical and Biomolecular Engineering, University of Notre Dame, Notre Dame, Indiana 46556, USA

(Received 25 January 2012; accepted 26 March 2012; published online 13 April 2012)

Accurate and efficient prediction of melting points for complex molecules is still a challenging task for molecular simulation, although many methods have been developed. Four melting point computational methods, including one free energy-based method (the pseudo-supercritical path (PSCP) method) and three direct methods (two interface-based methods and the voids method) were applied to argon and a widely studied ionic liquid 1-n-butyl-3-methylimidazolium chloride ([BMIM][Cl]). The performance of each method was compared systematically. All the methods under study reproduce the argon experimental melting point with reasonable accuracy. For [BMIM][Cl], the melting point was computed to be 320 K using a revised PSCP procedure, which agrees with the experimental value 337–339 K very well. However, large errors were observed in the computed results using the direct methods, suggesting that these methods are inappropriate for large molecules with sluggish dynamics. The strengths and weaknesses of each method are discussed. © *2012 American Institute of Physics*. [http://dx.doi.org/10.1063/1.3702587]

I. INTRODUCTION AND BACKGROUND

Melting point T_m is one of the most fundamental yet important properties for a compound.[1–6] Many methods have been developed for the computation of melting points. These methods can be categorized into two groups. The first group, which will be referred to as "direct" methods, include the hysteresis method,[3,4,7,8] the voids method,[9–15] and solid-liquid interface-based methods.[16–22] These approaches all involve the direct simulation of the melting process in a dynamical manner. They are relatively easy to apply but their accuracy can be limited. The second category of methods will be referred to as free energy methods, which are in principle more rigorous than direct methods but are generally more complicated to apply. This group of methods include Hoover and Ree's single-occupancy cell method,[23,24] Frenkel and Ladd's Einstein crystal method,[25] and the λ-integration method developed by Grochola and co-workers.[26,27] This latter method was extended by our group[28,29] and will be referred to as the pseudo-supercritical path (PSCP) method.

Probably the most straightforward way to calculate the melting point is to carry out molecular dynamics simulations of a perfect lattice at increasing temperatures. The temperature at which the lattice breaks down corresponds to the melting point. However, the existence of superheating, or the so-called hysteresis phenomenon, results in a significant overestimation of the melting points even for simple monatomic molecules.[13] Similarly, when a liquid is cooled down, the phase change temperature is underestimated due to the existence of supercooling. Based on the homogeneous nucleation melting theory, the hysteresis method was developed, in which the thermodynamic melting point is related to superheating and supercooling behavior as $T_m = T^+ + T^- - \sqrt{T^+T^-}$ where T^+ and T^- are the observed phase change temperatures when heating up a crystal and cooling down a liquid in a simulation, respectively.[3,4,7] It is usually easy to get T^+ from a molecular dynamics simulation, but except for simple monatomic molecules, T^- is extremely hard to obtain because crystal nucleation is a rare event. T^- can be approximated by the corresponding glass transition temperature[8] T^g, but the application of the hysteresis method is still limited due to its relatively low accuracy.

Defects always exist in crystals and are found to lower the observed melting point.[9,10,30–33] Based on this observation, the voids method was developed. This method has been well summarized in a recent review paper.[34] Briefly, defects, or voids, are created in a perfect crystal. Constant pressure simulations are then carried out with the temperature gradually increased in one trajectory or alternatively, a series of constant pressure simulations are carried out with each trajectory having a different but fixed temperature. In each simulation, the melting point is estimated to be the temperature at which a discontinuity in system properties such as density, potential energy, or atomic root mean squared displacement (RMSD) occurs. The observed melting points decrease with increasing void density. As the void density increases further, it is often observed that the apparent melting point becomes independent of the void density. The temperature at which this occurs is taken as the thermodynamic melting point.

The physical reason for the reduction in apparent melting point with increasing void density is due to the fact that this (and all direct methods) require the nucleation of a liquid region within the crystal phase. The voids serve to lower the nucleation free energy barrier, thereby enabling melting to be

a)Author to whom correspondence should be addressed. Electronic mail: ed@nd.edu.

observed on the time- and length-scales accessible to molecular dynamics simulation.

An alternative way of lowering the nucleation free energy barrier is to simulate a solid-liquid interface.[16,17] At least two procedures based on this concept have been developed.[19] One procedure involves the generation of a collection of constant pressure and constant temperature (NPT) ensemble trajectories, with each trajectory at the same pressure but a different temperature. The melting point is taken as the temperature at which a discontinuity in the system properties (such as density) occurs. This interface/NPT method is therefore very similar to the hysteresis and voids methods, but relies on the solid-liquid heterogeneous interface to lower the nucleation barrier. The other procedure utilizes a series of constant volume and constant energy (NVE) simulations. In this interface/NVE procedure, a solid and liquid interface is created and equilibrated at a given temperature and volume (NVT) followed by production simulations in the NVE ensemble. Once the system reaches equilibrium in the NVE ensemble, a density perturbation is applied by changing the simulation box size. In response, the total system energy will either increase or decrease. A new NVE simulation is then carried out on the perturbed system, and part of the solid will melt or part of the liquid will crystallize, causing a redistribution of the potential energy and kinetic energy until a new equilibrium is reached. If the perturbation is small, the liquid-solid interface remains. The average temperature and pressure of the system are recorded, thereby giving one point on the solid-liquid coexistence curve. Additional perturbations are applied until a set of equilibrium pressure/temperature points are obtained. The temperature on the curve for a given pressure corresponds to the melting point of the compound at that pressure.

The formal thermodynamic definition of the melting point is the temperature at which the crystal phase and liquid phase of a compound share the same free energy. As the name implies, free energy-based methods involve the explicit computation of free energy and so generally avoid nucleation phenomena. Similar to direct methods, avoiding errors caused by hysteresis phenomena associated with the first-order phase transition between the liquid and crystal phases is one of the main concerns in the development of these approaches. Thermodynamic integration is typically used to compute the free energy change along a carefully designed path.

In the single-occupancy cell method of Hoover and Ree,[23,24] the real system under study is connected to a low density lattice in which each particle occupies an individual cell and the free energy is analytically known. At high enough density, the interaction between the particles and the cell walls are negligible and the real system is restored. The solid-liquid phase change is completely avoided or controlled to occur at low density so that hysteresis does not occur. In a similar spirit, Frenkel and Ladd's Einstein crystal method[25] couples the solid phase to an Einstein crystal, for which the free energy is known analytically. The liquid is coupled in the same manner to an ideal gas or some other reference state with known free energy. Once the free energy differences between the actual solid and liquid and the reference states are known, the free energy difference between the solid and liquid can be computed indirectly. For the PSCP method,[26,28] the solid and liquid states are connected directly by intermediate states, so no analytical reference states are required. The intermolecular interactions are scaled down in the intermediate states and the phase change is controlled to occur in a reversible way so that the error caused by superheating is minimized. This method has been applied to a number of molecular systems of varying complexity.[29,35]

The PSCP method is an example of an "inter-phase" approach where the two coexisting phases of interest are linked directly. Another example of this is the "phase switch" method.[36] This method works by transforming between the liquid and solid phases via "gateway" states.[37] The free energy difference between the two phases is computed as a ratio of probabilities of the frequency of visits made to the two states. The method has been applied successfully to simple systems, but it is unclear how to apply it to complex multi-atom molecular systems. A similar approach based on an extension to the single-occupancy cell method has been proposed recently by Orkoulas and co-workers.[38–40]

In addition to the above mentioned molecular simulation methods, other simulation[41–45] or quantitative structure-property relationship (QSPR) models[46–52] have been developed for the prediction or correlation of melting points. The QSPR models have been applied to systems including ionic liquids. Relative to the molecular simulation based approaches, the QSPR methods are simple to apply. However, the accuracy of these methods is usually limited and highly depends on the availability of training sets of experimental data to parameterize the model. The parameters are generally valid only for compounds similar to those in the training set, which makes these models less useful when new compounds are being developed.

Despite all the activity in this area, predicting melting points using computational methods remains an extremely challenging problem. Most of the atomistic simulation methods have been validated for relatively simple systems such as the Lennard-Jones fluid. It is important to understand how these different approaches perform when applied to more complex molecules.

Recently, several direct methods for melting point computation were compared by Zhou and co-workers.[53] The voids method and the interface/NVE method were suggested to be favorable approaches. However, these two methods were likely improperly applied in the study. For the voids method, only one simulation with 16 voids was carried out. Previous studies[54–56] have shown that a series of simulations at different void densities should be used. Since the apparent melting point depends on void density, the use of a single arbitrary void density is not justified. In the interface/NVE simulation, Zhou and co-workers reported that they started from a configuration equilibrated under NPT conditions, but then only ran a single NVE trajectory following the perturbation. The final temperature they observed was taken as the melting point. Since pressure and temperature are coupled in the NVE ensemble,[18,57] the equilibrium "melting point" temperature observed from the NVE simulation is at whatever the average pressure was during the simulation. The final pressure from the simulation was not reported by Zhou and co-workers. Given the perturbation to the system, however, it is

reasonable to believe that the final pressure is not equal to one atmosphere, the value set during the NPT equilibration. The conclusions drawn by Zhou *et al.* must therefore be considered premature.

The objective of the present work is to perform a rigorous comparison of three of the popular "direct" approaches with the PSCP method for a simple Lennard-Jones model of argon and a complex atomistic model of the ionic liquid, 1-n-butyl-3-methylimidazolium chloride [BMIM][Cl]. It has previously been shown[26,28] that the PSCP method gives results for the Lennard-Jones fluid and a model for a simple molten salt that are consistent with the Frenkel-Ladd method, and so it is assumed that this method provides the correct baseline results consistent with free energy-based techniques. Systematic comparisons are made between the different methods and the performance of each method is discussed. In addition, a revised procedure is suggested for the PSCP method, which provides a more robust way of calculating the melting point of complex molecules.

II. SIMULATION PROCEDURE AND DETAILS

The force field for argon was taken from Ref. 58. The all-atom force field from our previous study[59] was used for the cation [BMIM] with the anion [Cl] parameters taken from Jensen and Jorgensen.[60] This combination has been shown to yield reliable results for both the crystal and liquid phases of [BMIM][Cl].[35] All the molecular dynamics simulations were carried out using the LAMMPS package[61] with periodic boundary conditions. A time step of 1 fs was used. Long range electrostatic interactions were calculated using the Ewald/n method[62] with real space cutoff shifted between 10.5 Å and 12 Å. The Nosé-Hoover thermostat and barostat method[63] was applied to control the temperature and pressure. The pressure was fixed to be one atmosphere in all constant pressure simulations with isotropic volume fluctuations for the liquid phase and anisotropic cell for the solid/lattice phase.

A. The pseudo-supercritical path (PSCP) method

The PSCP procedure consists of two steps. Details of the procedure can be found elsewhere.[29,35] Briefly, in the first step, the free energy of pure liquid and pure solid phases as a function of temperature are calculated from a series of constant pressure and constant temperature (NPT) simulations using the Gibbs-Helmholtz equation

$$\frac{G}{RT} - \left(\frac{G}{RT}\right)_{ref} = \int_{T_{ref}}^{T} -\frac{H}{RT^2} dT, \tag{1}$$

where T_{ref} is an arbitrary reference temperature.

The absolute free energy difference between the liquid (L) and crystal (C) phases at a reference temperature is then determined in the second step using the thermodynamic integration method along a PSCP. As shown in Figure 1, along the PSCP, the liquid and crystal phases are connected by three intermediate states: the weakly interacting liquid (WL), the dense weak fluid (DWF), and the weakly interacting crystal (WC).

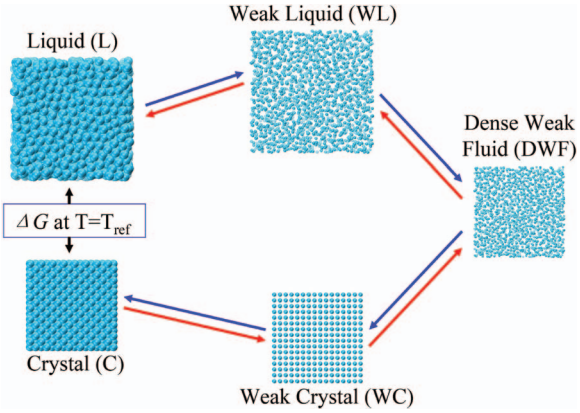

FIG. 1. A schematic of the pseudo-supercritical path for melting point calculations.

The WL state is realized by scaling the intermolecular potential energy based on the following equation:

$$U(\lambda) = [1 + \lambda(\eta - 1)]^m U^{vdW} + [1 + \lambda(\eta - 1)]^n U^{elec}, \tag{2}$$

where U^{vdW} and U^{elec} are van der Waals and electrostatic components of the potential energy, respectively, η is a scaling parameter having value of $0 < \eta < 1$, m and n are positive integer exponents, and λ is a coupling parameter that ranges from 0 to 1. The Helmholtz free energy change associated with this step is computed as

$$\Delta A = \int_0^1 \left\langle \frac{\partial U}{\partial \lambda} \right\rangle_\lambda d\lambda. \tag{3}$$

In the second step along the path, the weak liquid is converted to a dense weak fluid. The box volume is changed from the average liquid phase volume V^L to the average crystal phase volume V^C at the reference temperature. The corresponding free energy change is given by

$$\Delta A = \int_{V^L}^{V^C} -\langle P \rangle dV. \tag{4}$$

In the third step, the dense weak fluid is converted to a weak crystal by turning on an external tethering potential, the role of which is to help the molecules find their sites corresponding to the crystal configuration. The tethering potential has the form

$$U_{tether} = -\lambda \sum_i \sum_j a_{ij} exp\left(-b_{ij} r_{ij}^2\right). \tag{5}$$

The positions of these Gaussian wells are based on the average atomic coordinates in the crystal phase. The well depth and width are controlled by parameters a_{ij} and b_{ij} so that the atoms under the tethering potential experience the same thermal fluctuations as in the crystal phase. In the last step, the weak crystal is converted to the crystal phase by turning off the tethering potential and turning back on the full intermolecular interactions. The total potential energy for this step is

$$U(\lambda) = [\eta + \lambda(1 - \eta)]^m U^{vdW} + [\eta + \lambda(1 - \eta)]^n U^{elec} - (1 - \lambda) \sum_i \sum_j a_{ij} exp\left(-b_{ij} r_{ij}^2\right) + U^{NS}, \tag{6}$$

where U^{NS} denotes all potential energy terms that are not scaled or affected along the PSCP path. The free energy changes associated with the third and fourth steps are calculated with thermodynamic integration via Eq. (3).

A 2048 atom system was used in the simulations of argon and 108 ion pairs were used for [BMIM][Cl]. The free energy curves for the single phase systems were generated from NPT ensemble simulations between 65 K and 95 K for argon and between 300 K and 400 K for [BMIM][Cl] under one atmosphere. A 2 ns trajectory was generated at each temperature and the last 1ns was used for analysis. In each step along the PSCP path, in order to compute the free energy change using the thermodynamic integration method, $\langle \frac{\partial U}{\partial \lambda} \rangle_\lambda$ or $\langle P \rangle$ was calculated with nine λ values or box volumes in addition to initial and final states. A 2 ns NVT ensemble simulation at a reference temperature of 90 K for argon and 380 K for [BMIM][Cl] was carried out at each λ or V value and the last 1ns was used for analysis. Parameters m, n, and η were chosen as 1, 2, and 0.1, respectively.[35]

B. Interface methods

The solid-liquid co-existing interface simulation system for argon was prepared by putting a perfect fcc lattice containing 2048 atoms and a pre-equilibrated liquid box in contact along the Z-direction.[18] The liquid box contained 2048 atoms and had a cubic shape during the equilibration. The cubic box was deformed before placing it in contact with the solid box so that its X and Y lengths matched those of the crystal box. An energy minimization was then carried out to remove high energy contacts between the two phases.

The preparation of the [BMIM][Cl] solid-liquid interface system followed a previous procedure.[19] A 3 × 3 × 8 supercell, containing 288 ion pairs and a total of 7488 atoms, was generated from its experimental crystal structure.[64] A 1 ns NPT ensemble simulation was carried out on the whole system at a temperature much higher than the experimental melting point (1000 K was used in the current work). During this stage, molecules located in the center part of the box were fixed to their initial positions, while molecules on both ends of the box were allowed to melt. This system was then minimized with the atoms in the central part of the box fixed. Another energy minimization followed with all atoms free to move. This resulted in a simulation box with two solid-liquid interfaces.

As mentioned in the Introduction, there are two procedures to determine the melting point with solid-liquid interface simulations. In the NPT ensemble procedure (interface/NPT), trajectories were generated for each temperature between 65 K and 95 K with 5 K intervals for the argon system. Simulations with 1 K intervals were added near the expected melting point. For [BMIM][Cl], simulations were carried out between 300 K and 700 K with 50 K intervals. Each trajectory was 5 ns in length and the system volume (inverse of density) was averaged for the last 3 ns.

In the interface/NVE procedure, the argon system was equilibrated for 200 ps in the NVT ensemble at four different temperatures, 80 K, 83 K, 85 K, and 88 K, respectively, to prepare four different initial configurations. Simulations started from each of these configurations were carried out in the NVE ensemble. Trajectories of 1 ns length were generated followed by a perturbation to the box by increasing the Z-dimension length by a 0.2 Å. The last 600 ps of each trajectory was used to calculate the average temperature and pressure.

For [BMIM][Cl], three initial configurations were prepared at 300 K, 320 K, and 340 K, respectively. Each NVE trajectory was 5 ns long and the last 3 ns was used for analysis. The simulation box was increased by 0.1 Å in the Z-direction as a perturbation.

C. Voids method

The simulation for argon was started with a perfect fcc lattice containing 2048 atoms. Voids were created by the removal of a number of atoms, 50, 100, 200, 300, and 400, respectively, from one corner of the simulation box. Previous work has shown that the way the voids are created does not affect the calculated melting point.[13] Constant pressure simulations were carried out for each system with the temperature linearly increased from 65 K to 100 K during a 2 ns trajectory by rescaling atomic velocities every 100 steps. System properties such as density, per molecule energy, and other well defined quantities can be used to monitor the evolution of the system. It has been shown that melting points determined using any of these quantities are consistent with each other.[54,55] The system density was used in the current study. The temperature at which a sudden density decrease occurred was considered the melting point in that trajectory.

For [BMIM][Cl], the simulation system was built up by reproducing its orthorhombic experimental crystal structure[64] unit cell by 4, 4, and 5 in the X, Y, and Z directions, respectively. The initial simulation box contained 320 [BMIM][Cl] pairs for a total of 8320 atoms. Up to 40 ion pairs were then randomly removed.[54] To allow enough time for the system to equilibrate, a 1 ns NPT ensemble trajectory was generated at each temperature between 250 K and 600 K with 50 K intervals. Longer trajectories were generated in some cases to assure the convergence of the simulation. The system density was calculated based on the last 500 ps of each trajectory to monitor the melting of the crystal.

III. RESULTS AND DISCUSSIONS

A. Computed T_m for argon

Using the PSCP method, the enthalpy as a function of temperature was obtained from NPT simulations on pure solid and pure liquid phases. The corresponding free energies were computed using Eq. (1) and are shown in Figure 2. The free energy difference between solid and liquid phases was then calculated at 90 K via the pseudo-supercritical path. The thermodynamic integration curve for each step is shown in Figure 3. The total free energy difference at 90 K was found to be 0.0233 Kcal/mol. The free energy curves of the liquid and solid phases were shifted accordingly and the melting point

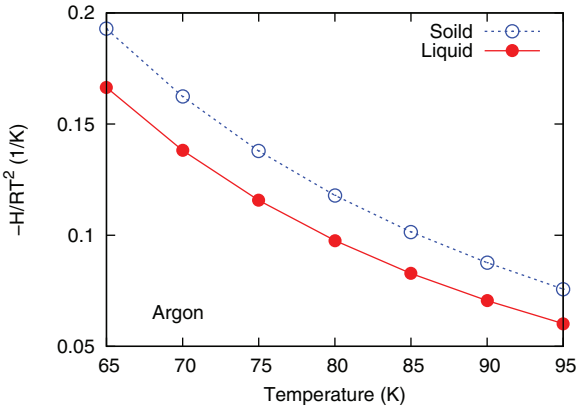

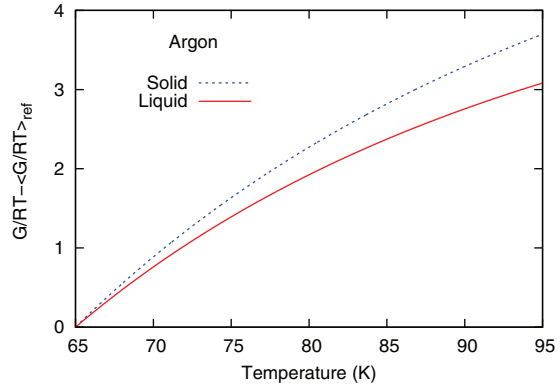

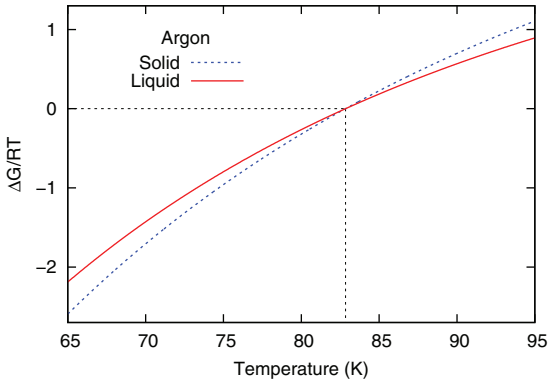

FIG. 2. The calculated enthalpy (top panel) and free energy (middle panel) against temperature for pure argon liquid and solid phases. The free energy difference between solid and liquid phases ΔG was computed to be 0.0233 Kcal/mol at 90 K and the shifted free energy curves are shown in the bottom panel. The melting point was determined to be 82.8 K.

was computed to be 82.8 K (see Figure 2 bottom panel). This agrees with experimental melting point[65] of 83.81 K almost perfectly.

The accuracy of the PSCP method depends on the assumption that the PSCP path is reversible. To test the validity of this assumption, the free energy difference ΔG_{ref} between the crystal phase and liquid phase of argon was also computed by reversing the PSCP path (starting from the solid phase and ending in the liquid phase). The corresponding simulation results are shown in Figure 4. It is clear by comparing Figure 4 to Figure 3 that the thermodynamic integration curves agree with each other very well (except for the opposite sign) for each of the corresponding steps. The free energy change for each step is summarized in Figure 5. The contribution from each step to ΔG_{ref} was found to be the same when computed in either direction. As expected, the same melting point of 82.8 K was determined when the direction of the path was reversed, thereby confirming the reversibility of the PSCP path for argon.

For the NPT interface based method, the average equilibrium volumes obtained from the simulations are shown in Figure 6. The solid-liquid interfacial system was allowed to evolve during the NPT simulation. Because the introduction of the crystal-liquid interface decreases the free energy barrier of the melting of crystal or freezing of liquid, at a given temperature the simulation cell converted to either a complete crystal or a complete liquid during the simulation. As a result, a sharp volume increase (or density decrease) was observed between 82 K and 83 K, which corresponds to the melting temperature, consistent with the PSCP melting point of 82.8 K.

The calculation results using the interface/NVE method are shown in Figure 7. In contrast to the interface/NPT method, the crystal-liquid interface was maintained during these simulations so that the equilibrium pressure and temperature from each simulation corresponds to a point on the crystal-liquid coexistence curve. When the NVE simulation started from configurations prepared using NVT simulations at 83 K or 85 K, the equilibrium P-T curves crossed the P = 1 atm line at T = 82.5 K and T = 82.9 K, respectively, ending up with the average melting point of 82.7 K. When the initial configuration was prepared at a temperature far from the experimental melting point, the equilibrium P-T points from the NVE simulations do not directly cross with the P = 1 atm line. However, as shown in the lower panel in Figure 7, P-T points from all four initial configurations can be fit by a single line, which yields a melting point of T = 82.8 K at P = 1 atm, consistent with the average value computed using the two curves that do cross with P = 1 atm line, and exactly matches the PSCP result.

The apparent melting point as a function of the number of voids in the simulation box is shown in Figure 8. When a perfect crystal (with zero voids) is heated, the apparent melting point was 99.6 K, 19% higher than the experimental value[65] of 83.81 K due to superheating. The apparent melting point decreases with increasing number of voids and reaches a flat region when around 100 voids are present. An average value of 89.4 K, determined from the flat region of Figure 8 was taken as the predicted melting point for argon using the void method. This is about 7 K higher than the experimental value and the values calculated using other methods but is consistent with previous results using the same method.[13]

As summarized in Table I, for this simple system, the computed melting points using all four methods agree very well with each other and with the experimental value[65] of 83.81 K with the largest error observed in the voids method. It can therefore conclude that any of these methods are appropriate to use for a simple system such as the Lennard-Jones fluid.

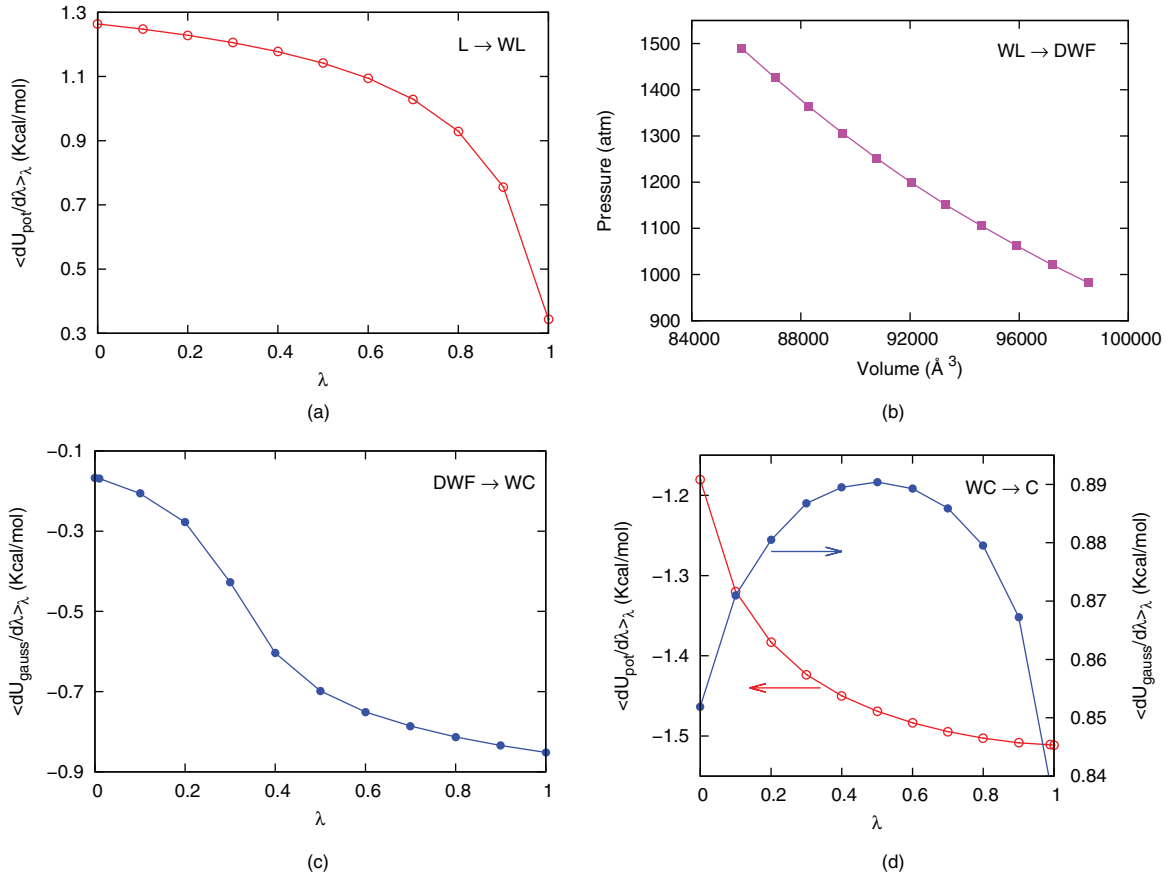

FIG. 3. The thermodynamic integrations for each step along the PSCP path calculated for argon at 90 K. The sum of all integration terms gives the free energy difference between solid and liquid phases at the reference temperature.

B. Computed T_m for [BMIM][Cl] using the PSCP procedure

The applicability of the four methods for computing the melting point of the ionic liquid [BMIM][Cl] was then examined. Following the conventional PSCP procedure described earlier, the melting point of [BMIM][Cl] was found to be 158 K, much lower than the experimental value of 337–339 K (Ref. 64 and 66) and at odds with an earlier calculation from our group.[35] Upon further investigation, it was found that the WC state at the end of the third step of the cycle was not achieved. Instead of the ordered crystalline state, the actual state at the end of this step was somewhat disordered. As a consequence, the final step (WC → C) did not result in the formation of the desired crystalline state. Because of this, the free energy computed during the cycle was not between the crystal and the liquid, but rather was between a disordered "glassy" state and the liquid. The free energies for each step in this path are shown in blue in Figure 9. Consequently, the apparent melting point of 158 K is not the true melting point.

For multi-atomic molecules, due to the huge number of intra- and inter-molecular degrees of freedom, the disorder-order transition is a rare event even with the application of tethering potentials as in the current work. The degree to which the path from the dense weak fluid (DWF) to the weak crystal (WC) actually reaches the WC state depends on the length of the trajectory. For this system, which has extremely slow dynamics, it is most likely that a glassy state will result. Previous results[35] achieved estimates of the melting point of [BMIM][Cl] using the PSCP method that were close to the experimental value, presumably because the WC and C configurations were close to the actual crystalline state. There is no way of assuring this, however, and so the path shown by the blue arrows in Figure 1 is not recommended. As an alternative, the free energy difference ΔG_{ref} was computed in the reverse order (C → L), as shown in red arrows in Figure 1. The transition from the crystal phase to the liquid phase is driven by entropy and it is easier to achieve in a simulation.

Using the revised procedure (starting from crystal phase), the melting point of [BMIM][Cl] was computed to be 320 K, which agrees well with the experimental value of 337–339 K.[64,66] The free energy change computed for each step is shown in Figure 9 together with results calculated using the original procedure (starting from liquid phase). The free energy changes for steps L-WL and WL-DWF are the same regardless of the direction of the thermodynamic integration. The potential energy of the state at the end of the C → L path was the same as the potential energy of the liquid at the beginning of the L → C path, confirming that the equilibrium liquid was reached. For the DWF-WC step, however, the free energy change was found to be larger (in its absolute value) when integrated from WC to DWF than from DWF to WC (see Figure 9). This is consistent with the observation that the ordered WC state was actually not reached at the end of

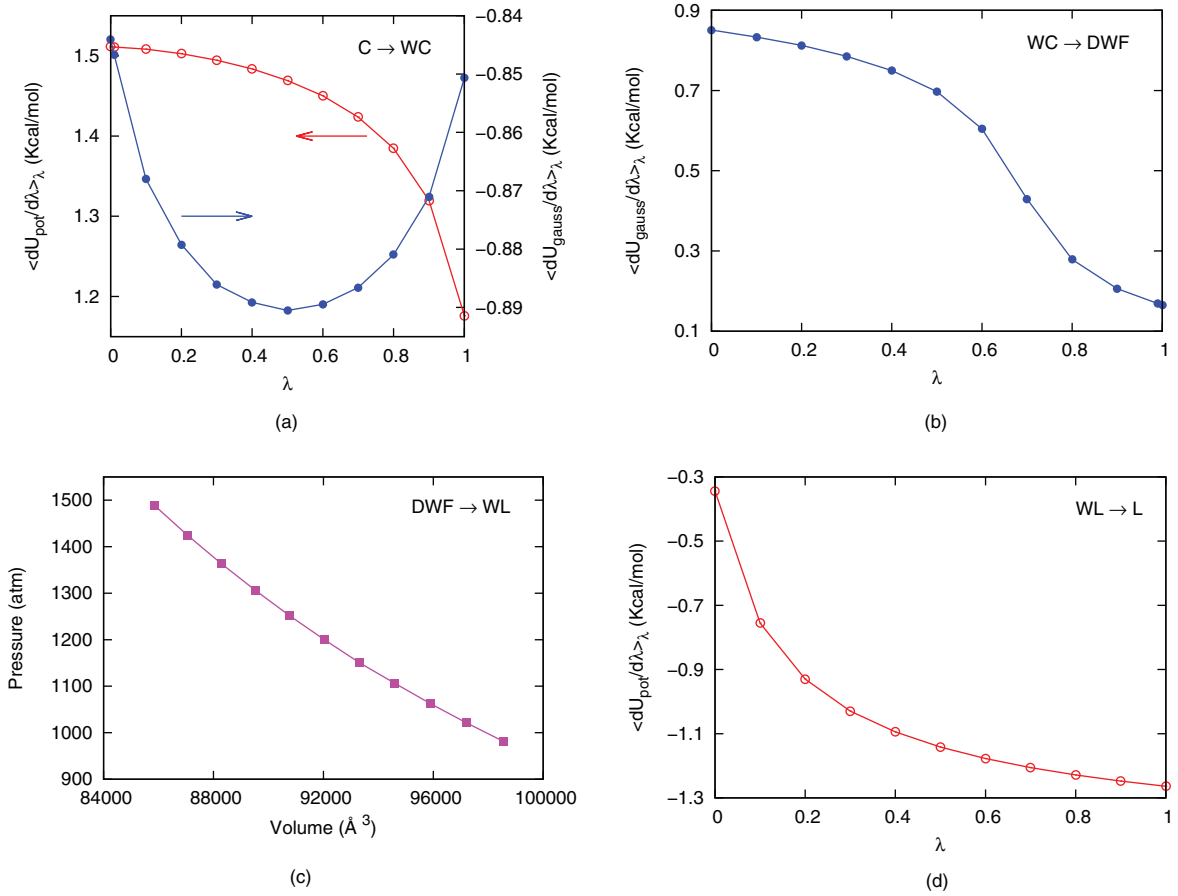

FIG. 4. The thermodynamic integrations for each step along the PSCP path for argon at 90 K computed by starting the simulation from the solid state. The computed results for each step agree with the corresponding step shown in Figure 3 where the simulation was started from liquid phase (note the difference in sign). Essentially, the same free energy difference ΔG was obtained from both calculations, confirming the reversibility of the PSCP path.

the DWF to WC path. Similar behavior was observed for the C-WC step. These "incomplete" paths are shown with dotted lines in Figure 9.

It has been observed previously that the strength of the tethering potential affects the accuracy and efficiency of the PSCP calculation.[35] The impact different tethering potentials have when using the C → L integration path was tested by carrying out simulations with different tethering potential strengths. In addition to full strength (scaled by 1.0), the tethering potential strength was scaled by 0.7, 0.5, 0.3, 0.1, and 0.0 (no tethering potential). The results for each step and the estimated melting points are summarized in Table II. For the

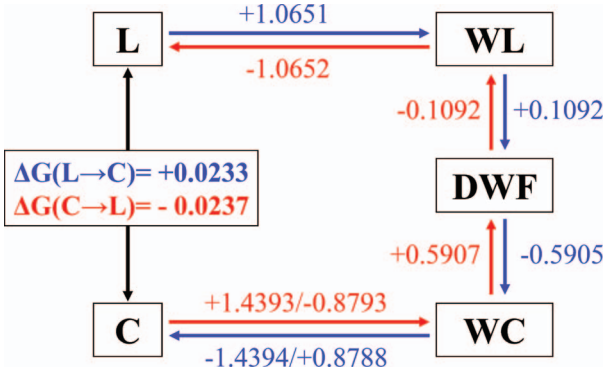

FIG. 5. The free energy difference (in Kcal/mol) between states along the PSCP path computed for argon at 90 K by starting the simulations from the liquid phase (blue) or the solid phase (red). The two numbers for the C-WC step are for contributions associated with scaling down the intermolecular interaction and the turning on/off of the tethering potential, respectively. The computed free energy change for each step along the path is independent of direction that the thermodynamic integration was carried out, demonstrating the reversibility of the method. The same melting point of 82.8 K was predicted, regardless of the integration direction.

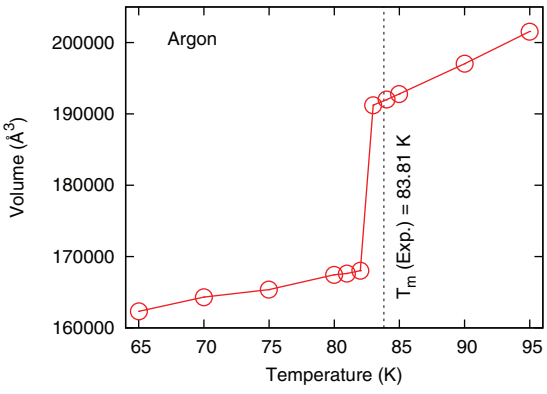

FIG. 6. The average equilibrium box volume of argon system as a function of temperature obtained from interface/NPT ensemble simulations. The melting point was determined to be between 82 K and 83 K where a sharp volume increase (or density decrease) was observed. The experimental melting point is indicated by a dashed line.

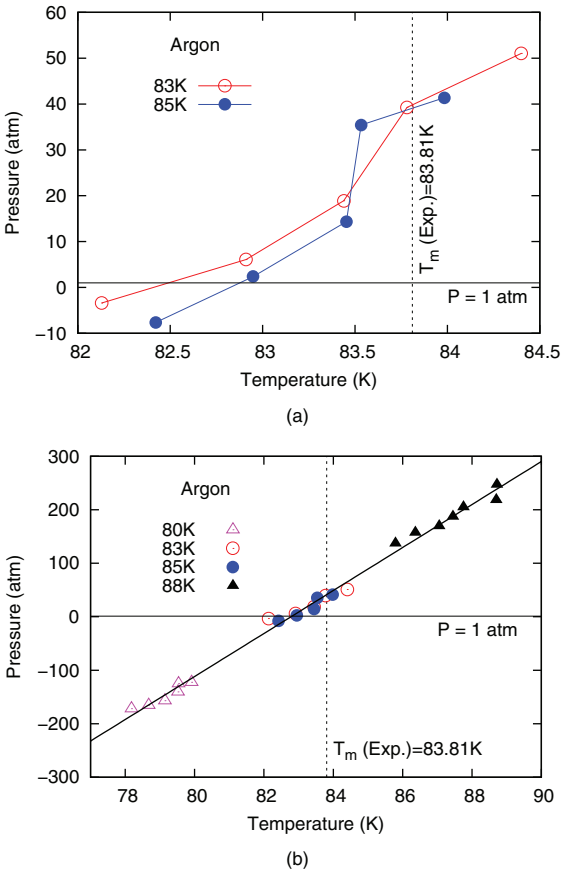

FIG. 7. Melting point calculation results for argon using the solid-liquid interface system with NVE ensemble simulations. The horizontal black line indicates the pressure of 1 atm and the vertical dashed line indicates the experimental melting point. TOP: The results when NVE simulations were started from 83 K and 85 K initial conditions. The equilibrated P-T curves cross with P = 1 atm line. The average melting point was found to be 82.7 K. BOTTOM: Simulation results from four different initial configurations prepared at different temperatures. All data points were fitted by a linear function and the melting point was determined to be 82.8 K.

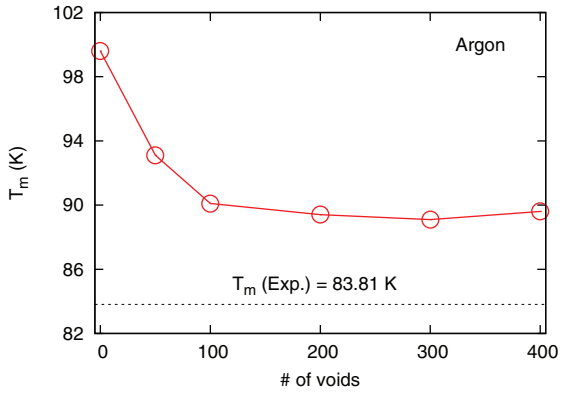

FIG. 8. The calculated melting points for argon using the voids method. The observed melting point decreases with increasing number of voids and reaches a flat region after 100 voids. The melting point was estimated to be 89.4 K by taking the average of the flat region. The experimental melting point is indicated by a dashed line.

TABLE I. Summary of calculated melting points (in K) for argon and [BMIM][Cl] using various simulation methods.

Method	Argon	[BMIM][Cl]
PSCP	82.8	320
Interface/NPT	82∼83	450∼500
Interface/NVE	82.8	-
Voids	89.4	-
Experiment	83.81[a]	337–339[b]

[a]Experimental melting point taken from Ref. 65.
[b]Experimental melting point taken from Refs. 64 and 66.

first step in the revised procedure (from C to WC), there are two contributions to the free energy difference, one associated with scaling down the intermolecular interaction and the other with the turning on of the tethering potential. The two numbers are listed separately in Table II. As shown in the table, when the scale factor ranges from 1.0 to 0.1, the computed melting points are almost the same although the free energy contribution from the first two steps vary. This suggests that when the integration is *started in the crystal phase* the melting point is insensitive to the strength of the tethering potential.

When the scaling factor was set to zero, however, which means the path goes from C to DWF directly without the WC intermediate state, the melting point was computed to be 487 K. The large error was caused by the fact that a first order phase change occurs during this step with a portion of the path having a significant interaction potential. In essence, the erroneous free energy computed in this way suffers from the same superheating phenomenon mentioned in the Introduction. When the weak crystal state is removed from the PSCP path, the crystal and the dense weak liquid states are connected directly and the phase change occurs at a stage with partial intermolecular interactions. The melting point

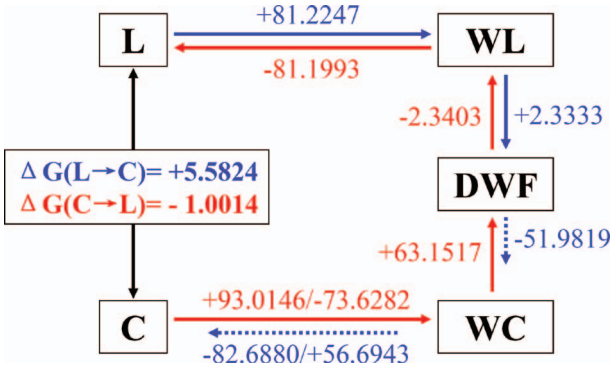

FIG. 9. The free energy difference (in Kcal/mol) between states along the PSCP path computed for [BMIM][Cl] at 380 K by starting the simulations from the liquid phase (blue) or the solid phase (red). The two numbers for the C-WC step are for contributions associated with scaling down the intermolecular interaction and the turning on/off of the tethering potential, respectively. The computed free energy change for L-WL and WL-DWF steps are the same (absolute values) no matter which direction the integration was carried out. For the other two steps, however, the free energy change was found to be larger if the integration was carried out from C to WC or from WC to DWF, respectively. This is consistent with the observation that when the simulation was carried out in the other direction, the ordered state was not reached so that the simulations ended up at some intermediate states (indicated by short dotted lines) and corresponding to smaller free energy change.

TABLE II. Individual contributions to the solid-liquid free energy difference (in Kcal/mol) for [BMIM][Cl] at 380 K and 1 atm using the revised PSCP method with scaled tethering potential strength. For the C → WC step, the first column refers to the intermolecular potential and the second column refers to the tethering potential (see text for detail).

Scale factor	C → WC		WC → DWF	DWF → WL	WL → L	ΔG	$T_m(K)$
1.0	94.0244	− 146.6393	135.1312	−2.3352	−81.1675	− 0.9864	320
0.7	93.4807	− 101.3602	90.4415	−2.3388	−81.2332	− 1.0100	319
0.5	92.9539	− 71.3701	60.9256	−2.3370	−81.2007	− 1.0283	318
0.3	92.1254	− 41.7483	32.2596	−2.3419	−81.1259	− 0.8312	328
0.1	90.2969	− 12.9334	5.2307	−2.3402	−81.2014	− 0.9475	322
0.0	85.1129[a]			−2.3432	−81.1652	1.6046	487

[a]C → DWF.

obtained in this case is in error due to an intermediate free energy barrier. This is confirmed by the fact that the computed melting point of 487 K is higher than the true value of 320 K but lower than ∼650 K estimate one obtains by heating up the perfect [BMIM][Cl] crystal (see below).

The simplified two intermediate states procedure (going directly from the crystal to a dense weak fluid without an intermediate weak crystal phase) was further tested on argon. The thermodynamic integration results computed in both directions were summarized in Figure 10. Even with the simple argon case, the free energy change computed going from C to DWF differs from that when going from DWF to C. Moreover, when the path goes from DWF to C, the crystal state C was actually not reached, but instead a disordered state was reached. This is reflected in the free energy changes shown in blue in Figure 10. When using the C to DWF step in the PSCP cycle, the computed melting point was 89.1 K, significantly higher than the true value. Like in the [BMIM][Cl] case, the computed melting point from the simplified PSCP path is higher than that from three intermediate states procedure (82.8 K) but lower than the value observed when a perfect crystal is heated (99.6 K). These results show the importance of including the weak crystal state in the PSCP path to ensure reversibility. It is not surprising that the intermediate WC state is needed to compute the free energy between the C and DWF states, as the "overlap" between the C and DWF states is small, and the use of additional intermediate states has been shown to be an effective means of overcoming this.[67,68]

C. Computed T_m for [BMIM][Cl] using the interface and voids methods

The interface/NPT method results for [BMIM][Cl] are shown in Figure 11. A sharp volume increase (or density decrease) of the simulation box was observed between 450 K and 500 K, suggesting that the melting point is in this range. Relative to the 650 K melting point estimate obtained from heating up a perfect crystal (see below), the introduction of the solid-liquid interface into the simulation system significantly decreased the superheating as well as the observed melting point. However, the melting point was still more than 100 K higher than the experimental value or the PSCP result, suggesting that the interface/NPT procedure is inaccurate for complex molecules with sluggish dynamics.

The interface/NVE simulations were carried out with three initial configurations prepared from NVT simulations at 300 K, 320 K, and 340 K, respectively. As shown in Figure 12, all the equilibrium P-T curves from the three simulations managed to cross with P = 1 atm line. Note that in each case, the pressure and energy of the systems reached a

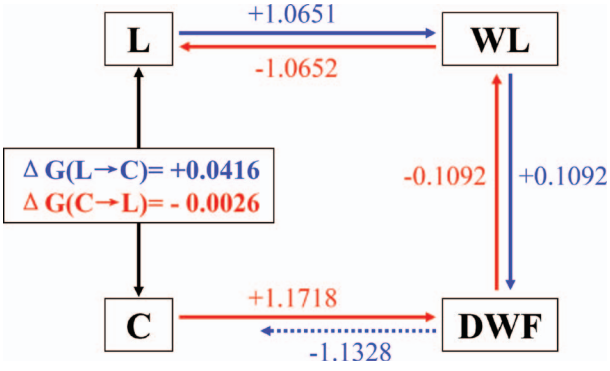

FIG. 10. The thermodynamic integration results (in Kcal/mol) computed along a two intermediate states PSCP path for argon at 90 K. Removing the weak crystal state from the path, the free energy change connecting the crystal and dense weak fluid states is different when the integration is computed in different directions. The crystal phase was actually not reached at the end of the simulation started from dense weak fluid state (indicated by short dotted line), indicating the importance of the weak crystal phase enforced by the tethering potential in ensuring the PSCP path to be reversible.

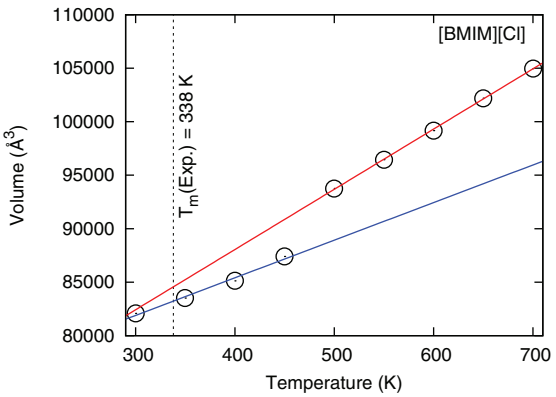

FIG. 11. The average equilibrium box volume of [BMIM][Cl] system as a function of temperature calculated from interface/NPT ensemble simulations. The melting of the crystal occurred between 450 K and 500 K, where a sharp volume increase (or density decrease) was observed. The two lines were fit to the solid and liquid phase data points, respectively. The experimental melting point is indicated by a vertical dashed line.

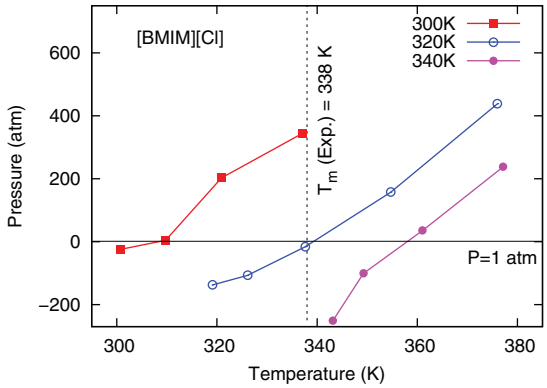

FIG. 12. Melting point calculation results for [BMIM][Cl] using the interface/NVE method. The horizontal black line indicates a pressure of 1 atm and the vertical dashed line the experimental melting point. NVE simulations were initiated from three configurations prepared at different temperatures. Three sets of P-T points crossed with P = 1 atm line at different temperatures varying by ~50 K, indicating strong dependence of the observed melting point on the initial simulation setup.

steady state value after the perturbation. The pressures and temperatures recorded in Figure 12 are averaged over 3 ns. However, there was a strong dependence of the predicted melting point on the initial simulation setup condition. The simulations started from a 300 K NVT configuration predicted the lowest melting point of 309 K, and the melting point obtained from the 340 K NVT initial configuration had the highest value of 358 K. When the NVE simulation was started from an initial configuration prepared at 320 K, the observed melting point was 339 K, in excellent agreement with the experimental value of 337–339 K.[64,66] However, the strong initial configuration dependence puts the reliability of the results under doubt. The melting point obtained from the 320 K initial configuration is more fortuitous than anything; without pre-knowledge of the approximate melting point, the interface/NVE method also does not appear to be reliable for complex molecules.

As mentioned above, the creation of solid-liquid coexisting interface in the simulation system significantly decreases the free energy barrier that causes superheating. As a result, the location of the solid-liquid interface in the argon simulation was able to move by crystallizing part of the liquid or melting part of the crystal at the interface on the time scale of the MD simulations. In [BMIM][Cl], however, as the melting process includes the rearrangement of both intra- and inter-molecular degrees of freedom and the interaction between [BMIM][Cl] ions are much stronger than the simple Lennard-Jones interactions between argon atoms, the melting and crystallization process is much slower. In other words, the interface is unable to move on the time scale of MD, thereby invalidating these interface methods. The temperature and pressure evolution observed in the simulations are mainly caused by the small rearrangement of molecules in each phase as the system box size changed. Extremely long trajectories on larger simulation systems are needed to observe interfacial motion for molecules such as [BMIM][Cl], which can easily reach the limit of available computational resources. Moreover, the anisotropy of molecular crystal makes such calculations even more complicated.

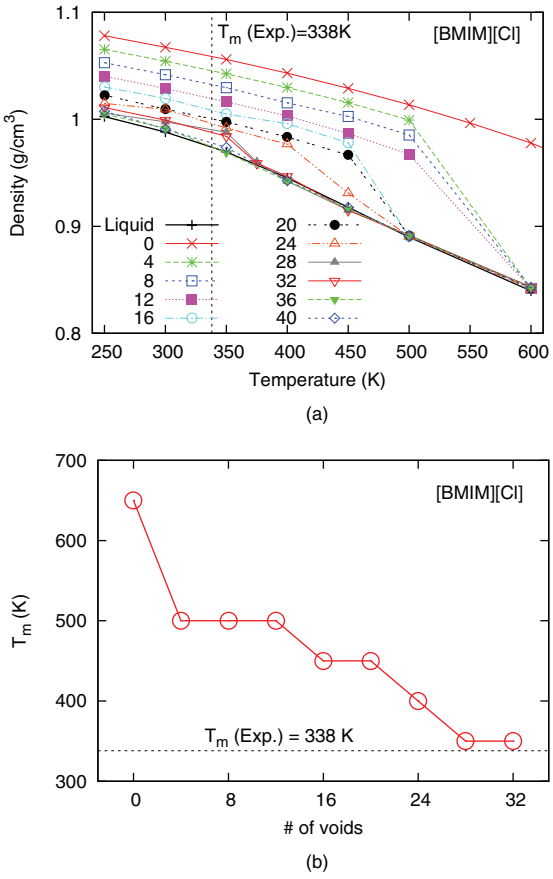

FIG. 13. The calculated melting point for orthorhombic [BMIM][Cl] using the voids method. The computed system density as a function of temperature is shown in the upper panel with the experimental melting point of 338 K indicated by a vertical line. The liquid phase density is included as solid black line. The observed melting point as a function of number of voids is shown in the lower panel. The dashed line indicates the experimental melting point. Unlike argon case, no clear flat region was observed before the crystal structure collapsed with more than 36 voids.

Finally, the voids method was applied to estimate the melting point of [BMIM][Cl]. The system density with various number of voids included in the box is shown in the upper panel in Figure 13. Similar to argon, significant superheating was observed for the perfect crystal (with zero voids) and the melting point was overestimated by more than 300 K.[64,66] With increasing void density, the crystal was observed to melt at decreasing temperature. When 36 or more voids were included in the crystal, the system density almost overlapped with that of the liquid phase over the entire temperature range, indicating that the crystal is unstable with this number of voids. With 28 or 32 voids, the system density is very close to that of liquid phase, especially at low temperature. An extra trajectory at 375 K was generated for these two cases. As shown in Figure 13, a phase change seems to appear between 350 K and 375 K, which is very close to the experimental melting point of 337–339 K for orthorhombic [BMIM][Cl].[64,66] If one knew that the melting point was 338 K, then one could simply "stop" adding additional voids when the density transition appeared at around the actual melting point. If, however, one uses the criterion that the actual melting point is the temperature at which the transition

becomes independent of the number of voids, then the picture is less clear. As shown in the lower panel of Figure 13, there are at least three "plateau" temperatures for this system (∼500 K, ∼450 K, and ∼350 K), unlike argon where a single transition was evident. Which one is the "correct" melting point? Given the fact that there is no clear cut transition temperature plateau for this system, it is concluded that the voids method is unable to reliably estimate the melting point for [BMIM][Cl]. We note that in order to ensure the convergence of the simulation, at least a 500 ps stable trajectory (no significant density change observed) was obtained before the density was computed; otherwise, longer trajectories were generated. As the dynamics tend to be slow for large molecules, however, it is likely that the observed melting points depend on the simulation length, which makes the application of the voids method complicated and the determination of melting point difficult.

The computed melting points for [BMIM][Cl] using all the different methods are summarized in Table I. The voids method and the interface based methods tested in this work failed to predict accurate results for [BMIM][Cl], despite working well for argon. The PSCP method, revised such that the integration path goes from the crystal phase to the liquid phase with the use of a weak crystal intermediate, performed well and gave a melting point of 320 K, in good agreement with the experimental value of 337–339 K.[64,66]

IV. SUMMARY AND CONCLUSIONS

Four different melting point computational methods were tested in the present work: the voids method, the interface/NPT method, the interface/NVE method, and the free energy based PSCP method. All employed molecular dynamics simulations and a systematic comparison was made on a neutral monatomic molecule (argon) and a multiatomic ionic liquids (1-n-butyl-3-methylimidazolium chloride or [BMIM][Cl]). For argon, the melting point was computed to be 89.4 K, 82 ∼ 83 K, 82.8 K, and 82.8 K from each method, respectively. All results agree well with the experimental melting point of 83.81 K.[65] On the other hand, there was a high degree of variability among the methods for the more complex ionic liquid.

For the PSCP method, a large error was found when the thermodynamic cycle was run in the liquid to crystal direction. This was caused by a failure to establish the ordered weak crystal state from the dense weakly interacting fluid within the limited length of the simulation. To overcome this, the thermodynamic integration cycle was carried out in the opposite direction (from crystal to liquid). This exploited the fact that the PSCP path is reversible in principle and on the time scale of a MD simulation it is easier to achieve a liquid phase from a crystal than a crystal from a liquid. Using the revised PSCP procedure, the melting point of [BMIM][Cl] was computed to be 320 K, in excellent agreement with the experimental value of 337–339 K.[64,66]

The reliability of the revised PSCP procedure was further tested with different tethering potential strengths. With the strength scaled by 1.0 through 0.1, the computed melting points were found to be nearly identical. These results indicate that the revised PSCP procedure is a robust approach for the computation of melting points even for complex molecules such as ionic liquids. When no tethering potential was applied (the tethering potential turned off), however, the melting point was predicted to be 487 K for [BMIM][Cl], ∼150 K higher than the experimental value. This suggests the importance of including the weak crystal state in the PSCP path and confirmed that the superheating was minimized along the PSCP path in which the crystal and liquid states are connected by three intermediate states. None of the other methods (voids, interface/NPT or interface/NVE) gave a reliable melting point for the ionic liquid. These results strongly suggest that the PSCP method yields accurate melting points for both simple and complex systems. While the agreement between the computed and experimental melting point for [BMIM][Cl] is not a guarantee of the accuracy of the method, the fact that it was shown to give perfect results for the simple argon system, coupled with the fact that each step in the PSCP cycle is consistent with a reversible path shows that this approach is superior to "direct" methods. This suggests that methods that are "dynamic" should not be used to estimate melting points for the complex systems with slow dynamics. Instead, free energy-based methods are recommended.

In summary, for simple systems such as argon, all methods tested in the current work predicted the melting point reasonably well. When the molecules become complex, however, the more rigorous free energy based pseudo-supercritical path method is necessary. The revised PSCP procedure was shown to be reliable and robust. The widely studied ionic liquid [BMIM][Cl] has served as a test case in the current work, but the procedure can be readily applied to other neutral and ionic molecules as well.

ACKNOWLEDGMENTS

This material is based upon work supported by the Air Force Office of Scientific Research under AFOSR (Award No. FA9550-10-1-0244) and by the Advanced Research Projects Agency - Energy (ARPA-E), (U.S.) Department of Energy (Award No. DE-AR0000094). Computational resources were provided by the Center for Research Computing (CRC) at the University of Notre Dame. We thank Dr. Saivenkataraman Jayaraman for his help in setting up the PSCP simulations.

[1] J. Lennard-Jones and A. Devonshire, Proc. R. Soc. London, Ser. A **169**, 317 (1939).
[2] Z. Jin, P. Gumbsch, K. Lu, and E. Ma, Phys. Rev. Lett. **87**, 055703 (2001).
[3] S. Luo, A. Strachan, and D. Swift, J. Chem. Phys. **120**, 11640 (2004).
[4] S. Luo and T. J. Ahrens, App. Phys. Lett. **82**, 1836 (2003).
[5] B. J. Siwick, J. R. Dwyer, R. E. Jordan, and R. D. Miller, Science **302**, 1382 (2003).
[6] K. Sokolowski-Tinten, C. Blome, J. Blums, A. Cavalleri, C. Dietrich, A. Tarasevitch, I. Uschmann, E. Forster, M. Kammler, M. Hom-von Hoegen, and D. v. d. Linde, Nature (London) **422**, 287 (2003).
[7] S. Luo, T. Ahrens, T. Cagin, A. Strachan, W. Goddard, and D. Swift, Phys. Rev. B **68**, 134206 (2003).
[8] L. Zheng, S. Luo, and D. Thompson, J. Chem. Phys. **124**, 154504 (2006).
[9] S. Phillpot, J. Lutsko, D. Wolf, and S. Yip, Phys. Rev. B **40**, 2831 (1989).
[10] J. Lutsko, D. Wolf, S. Phillpot, and S. Yip, Phys. Rev. B **40**, 2841 (1989).
[11] J. Solca, A. J. Dyson, G. Steinebrunner, B. Kirchner, and H. Huber, Chem. Phys. **253**, 253 (1997).

[12]J. Solca, A. J. Dyson, G. Steinebrunner, B. Kirchner, and H. Huber, J. Chem. Phys. **108**, 4107 (1998).
[13]P. Agrawal, B. Rice, and D. Thompson, J. Chem. Phys. **118**, 9680 (2003).
[14]P. M. Agrawal, B. M. Rice, and D. L. Thompson, J. Chem. Phys. **119**, 9617 (2003).
[15]G. Velardez, S. Alavi, and D. Thompson, J. Chem. Phys. **120**, 9151 (2004).
[16]J. Morris, C. Wang, K. Ho, and C. Chan, Phys. Rev. B **49**, 3109 (1994).
[17]A. B. Belonoshko, R. Ahuja, and B. Johansson, Phys. Rev. Lett. **84**, 3638 (2000).
[18]J. Morris and X. Song, J. Chem. Phys. **116**, 9352 (2002).
[19]S. W. Watt, J. A. Chisholm, W. Jones, and S. Motherwell, J. Chem. Phys. **121**, 9565 (2004).
[20]E. Schwegler, M. Sharma, F. Gygi, and G. Galli, Proc. Natl. Acad. Sci. U.S.A. **105**, 14779 (2008).
[21]S. Yoo, S. S. Xantheas, and X. C. Zeng, Chem. Phys. Lett. **481**, 88 (2009).
[22]S. Yoo, X. C. Zeng, and S. S. Xantheas, J. Chem. Phys. **130**, 221102 (2009).
[23]W. Hoover and F. Ree, J. Chem. Phys. **47**, 4873 (1967).
[24]W. Hoover and F. Ree, J. Chem. Phys. **49**, 3609 (1968).
[25]D. Frenkel and A. Ladd, J. Chem. Phys. **81**, 3188 (1984).
[26]G. Grochola, J. Chem. Phys. **120**, 2122 (2004).
[27]G. Grochola, J. Chem. Phys. **122**, 046101 (2005).
[28]D. Eike, J. Brennecke, and E. Maginn, J. Chem. Phys. **122**, 014115 (2005).
[29]D. Eike and E. Maginn, J. Chem. Phys. **124**, 164503 (2006).
[30]N. Ainslie, J. Mackenzie, and D. Turnbull, J. Phys. Chem. **65**, 1718 (1961).
[31]R. Cormia, J. Machenzie, and D. Turnbull, J. Appl. Phys. **34**, 2239 (1963).
[32]P. Stoltze, J. Norskov, and U. Landman, Phys. Rev. Lett. **61**, 440 (1988).
[33]G. Bilalbegovic, F. Ercolessi, and E. Tosatti, Surf. Sci. Lett. **258**, L676 (1991).
[34]S. Alavi and D. L. Thompson, Mol. Simul. **32**, 999 (2006).
[35]S. Jayaraman and E. J. Maginn, J. Chem. Phys. **127**, 214504 (2007).
[36]N. Wilding and A. Bruce, Phys. Rev. Lett. **85**, 5138 (2000).
[37]A. D. Bruce and N. B. Wilding, Adv. Chem. Phys. **127**, 1 (2003).
[38]G. Orkoulas and M. Nayhouse, J. Chem. Phys. **134**, 171104 (2011).
[39]M. Nayhouse, A. M. Amlani, and G. Orkoulas, J. Chem. Phys. **135**, 154103 (2011).
[40]M. Nayhouse, A. M. Amlani, and G. Orkoulas, J. Phys.: Condens. Matter **23**, 325106 (2011).
[41]D. A. Kofke, Mol. Phys. **78**, 1331 (1993).
[42]D. A. Kofke, J. Chem. Phys. **98**, 4149 (1993).
[43]R. Agrawal and D. A. Kofke, Mol. Phys. **85**, 43 (1995).
[44]E. A. Mastny and J. J. de Pablo, J. Chem. Phys. **122**, 124109 (2005).
[45]F. A. Escobedo, J. Chem. Phys. **123**, 044110 (2005).
[46]A. Katritzky, A. Lomaka, R. Petrukhin, R. Jain, M. Karelson, A. Visser, and R. Rogers, J. Chem. Inf. Comput. Sci. **42**, 71 (2002).
[47]D. Eike, J. Brennecke, and E. Maginn, Green Chem. **5**, 323 (2003).
[48]S. Trohalaki, R. Pachter, G. W. Drake, and T. Hawkins, Energy Fuels **19**, 279 (2005).
[49]N. Sun, X. He, K. Dong, X. Zhang, X. Lu, H. He, and S. Zhang, Fluid Phase Equilib. **246**, 137 (2006).
[50]I. Krossing, J. M. Slattery, C. Daguenet, P. J. Dyson, A. Oleinikova, and H. Weingaertner, J. Am. Chem. Soc. **128**, 13427 (2006).
[51]I. Krossing, J. M. Slattery, C. Daguenet, P. J. Dyson, A. Oleinikova, and H. Weingaertner, J. Am. Chem. Soc. **129**, 11296 (2007).
[52]U. Preiss, S. Bulut, and I. Krossing, J. Phys. Chem. B **114**, 11133 (2010).
[53]H. Feng, J. Zhou, and Y. Qian, J. Chem. Phys. **135**, 144501 (2011).
[54]S. Alavi and D. Thompson, J. Phys. Chem. B **109**, 18127 (2005).
[55]S. Alavi and D. Thompson, J. Chem. Phys. **122**, 154704 (2005).
[56]P. Agrawal, B. Rice, L. Zheng, G. Velardez, and D. Thompson, J. Phys. Chem. B **110**, 5721 (2006).
[57]S. Yoo, X. Zeng, and J. Morris, J. Chem. Phys. **120**, 1654 (2004).
[58]J. Gezelter, E. Rabani, and B. Berne, J. Chem. Phys. **107**, 4618 (1997).
[59]C. Cadena and E. J. Maginn, J. Phys. Chem. B **110**, 18026 (2006).
[60]K. P. Jensen and W. L. Jorgensen, J. Chem. Theory Comput. **2**, 1499 (2006).
[61]S. Plimpton, J. Comp. Physiol. **117**, 1 (1995).
[62]P. J. I. Veld, A. E. Ismail, and G. S. Grest, J. Chem. Phys. **127**, 144711 (2007).
[63]W. G. Hoover, Phys. Rev. A **31**, (1985).
[64]J. D. Holbrey, W. M. Reichert, M. Nieuwenhuyzen, S. Johnston, K. R. Seddon, and R. D. Rogers, Chem. Commun. **2003**, 1636.
[65]*CRC Handbook of Chemistry and Physics Internet Version 2012*, (Taylor & Francis, 2012).
[66]H.-O. Hamaguchi and R. Ozawa, Adv. Chem. Phys. **131**, 85 (2005).
[67]N. Lu, D. A. Kofke, and T. B. Woolf, J. Phys. Chem. B **107**, 5598 (2003).
[68]D. Wu and D. A. Kofke, J. Chem. Phys. **123**, 084109 (2005).